

EFFECT OF SYNTHESIS ON THE PURITY AND PARTICLE SIZE OF ZrB₂ POWDER

S. Gadakary^a, M. J. Davidson^b, R. Veerababu^c, A.K. Khanra^{a*}

^aDepartment of Metallurgical and Materials Engineering, National Institute of Technology, Warangal, India

^bDepartment of Mechanical Engineering, National Institute of Technology, Warangal, India

^cDefence Metallurgical Research Laboratory, Hyderabad, India

(Received 21 November 2014; accepted 01 September 2015)

Abstract

In the present investigation, an attempt has been made to prepare ZrB₂ powder by self-propagating high temperature synthesis (SHS) technique. The effect of synthesis on the purity and morphology of powder is investigated. A stoichiometric mixture of ZrO₂, H₃BO₃ and Mg powder is synthesised in a resistance heating tubular furnace with continuous flow of high pure argon gas. The synthesis is also carried out with NaCl as a diluent. The MgO is leached out from the as-synthesised powder. Phase analysis of powder is performed by X-ray diffraction (XRD). Laser beam scattering technique is used to measure the particle size distribution. The morphology of powder is characterized by scanning and transmission electron microscopes. The XRD results show the presence of significant amount of unreacted ZrO₂ phase in the product. The product is mixed with calculated amount of magnesium and boric acid and the mixture is synthesised further. There is a significant decrease of unreacted ZrO₂ in the product after double synthesis. The SEM images show the presence of agglomeration of fine particles, whereas the TEM images show the decrease of particle size after double synthesis. To understand the synthesis process, the individual synthesis of ZrO₂-Mg and H₃BO₃-Mg are also performed.

Keywords: Ceramics; SHS; Nanocrystalline; Zirconium Diboride; XRD; SEM; TEM

1. Introduction

Zirconium diboride (ZrB₂) is an ultrahigh-temperature ceramics class with a melting point of 3050°C. It has outstanding wear and corrosion resistance, high heat and electrical conductivity, and high hardness, a high melting point, good mechanical properties, chemical inertness, high thermal and electrical conductivities, and good resistance to erosion/corrosion [1]. Typical applications of ZrB₂ include cutting tools, crucibles for molten metal handling, high-temperature electrodes and high-temperature spray nozzles. ZrB₂ has also been used for refractory linings, electrodes and in microelectronics [2]. It is considered for use in extreme chemical and thermal environments related to hypersonic flight, space shuttle use and rocket propulsion [3]. ZrB₂ based ceramics are suitable candidates for high temperature applications in the future [4-5], for high temperature structural applications, such as sharp noses and leading edges of re-entry and hypersonic vehicles [6-9].

ZrB₂ powder can be synthesized mainly by the following methods: (i) solid-state reaction synthesis,

(ii) electrochemical synthesis, (iii) mechanochemical synthesis and (iv) self-propagating high-temperature synthesis [10]. ZrB₂ has been synthesized through various starting materials such as elemental Zr or its oxide, ZrO₂. Reaction between Zr and B elemental powders, metallothermic reduction of ZrO₂ and B₂O₃ by magnesium or boron, fused salt electrolysis; mechanochemical synthesis and combustion synthesis are some of the methods. Nano-size ZrB₂ powder is prepared by SHS through mixing of Zr and B elemental powders [1]. Zirconium diboride (ZrB₂) powders were synthesized by using ZrO₂, B₂O₃ and C (carbothermal reduction), ZrO₂ and B₄C (boron carbide reduction), and ZrO₂, B₄C and C (combined reduction) [2]. ZrB₂/ZrC/SiC precursors were prepared in a one-pot reaction of polyzirconoxanesal with boric acid and poly (methylsilylene) ethynylene[4]. Zirconium diboride (ZrB₂) nanoparticles were synthesized by sol-gel method using zirconium n-propoxide (Zr(OPr)₄), boric acid (H₃BO₃), sucrose (C₁₂H₂₂O₁₁), and acetic acid (AcOH) [10]. Formation of ZrB₂ by volume combustion synthesis (VCS) and mechanochemical process (MCP) from ZrO₂-Mg-B₂O₃ was studied by

* Corresponding author: asit@nitw.ac.in

Akgün et.al. [11]. Highly c-axis oriented ZrB₂ based ultrahigh temperature ceramics (UHTCs) were prepared via strong magnetic field alignment during slip casting, followed by spark plasma sintering [12].

In the present paper, the ZrB₂ powder is synthesized by SHS method. The main feature of the SHS process is that, it utilizes the high energy released during the exothermic chemical reaction of the reactants to yield a variety of inorganic materials. The reactants are initially ignited by an external source, then the reaction front will propagate within the solid with a certain velocity to complete the chemical reaction. The ignition time is very short and localized activation is sufficient, which enables the preparation of a large numbers of high-temperature advanced materials without employing any high temperature furnaces. The SHS offers wide range of applications for manufacturing several inorganic materials such as borides, carbides, nitrides, aluminides, silicides, hydrides, intermetallics, carbonitrides, cemented carbides, chalcogenides, composites [19], CoCrMoC [13], Fe–Ni Alloys [14], MoSi₂ powders [15] and ZrB₂–SiC composite powders [16]. Kamali et. al. have used the Low-Temperature Combustion Synthesis Process for production of Ti from TiO₂ [17]. TiB₂ is produced through SHS method in the recent years [18]. It has wide range of applications such as in abrasives, cutting tools, polishing powders, resistive heating elements, shape-memory alloys, high temperature intermetallic compounds, steel processing additives (nitrided ferroalloys), electrodes for electrolysis of corrosive media, coatings for containment of liquid metals and corrosive media, thin films and coatings, functionally graded materials and composite materials [20]. SHS method is also developed to be used in preparing dense ceramics and glasses by melt casting instead of conventional powder sintering [20-21]. This technique combines strong exothermic chemical reactions with a high gravity field, and offers an efficient and furnace free way for rapid production of bulk ceramic and glass materials. The main drawbacks of this process are to control the kinetics of reaction because of very fast process.

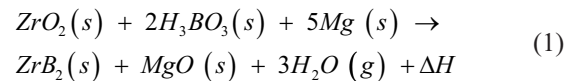
In the present investigation, an attempt has been made to produce the ZrB₂ powder by using alternative sources of raw materials and to investigate the kinetics of the process. Various morphologies of ZrB₂ particles are produced by controlling the process parameters. The synthesized powder is characterized by XRD and electron microscopes.

2. Experimental procedure

Zirconium oxide (ZrO₂) (> 99% pure, Loba Chemicals, India), boric acid (H₃BO₃) (99 % pure, Loba-Chemicals, India) and magnesium (99.9 % pure

and particle size <150 μm, Loba-Chemicals) were used for the synthesis of ZrB₂. The morphologies of ZrO₂ and Mg powders (Fig.1) reveal the presence of big chunky agglomerations of particles for ZrO₂ powder (Fig. 1a), whereas Mg powder (Fig. 1b) shows flaky shaped particles with surface cracks. The ZrO₂, H₃BO₃, and Mg mixture is taken as per the stoichiometric ratio as per the Eq. (1). The powders were mixed in a mortar mixer in order to make a uniform mixture. The mixture is then taken into a stainless steel boat. The boat is then kept in a tubular furnace (Systems control, Chennai, India). The furnace is continuously flown with the argon (99.99 % pure) such that Mg will not get oxidized. The mixture is then heated up to 750°C. The reaction took place at a temperature 720 ± 15°C. The mixture is then allowed to cool in the furnace. The reacted mixture contains black lumps with white layer on it. The lumps are then crushed to fine powder. The powder is then leached in the diluted hydrochloric acid (HCl), to leach out the MgO formed after the reaction.

After leaching process, the powder is separated by using filter paper and then dried in an oven.



The effect of NaCl addition is also studied on the synthesis of ZrB₂ powder. In the initial raw mixture, NaCl with 10 wt. % and 20 wt. % are added in order to control the process. The effect of NaCl addition is also observed on the resultant powder. The pyrolysis of mixture is found to be explosive in nature and deposition of fine white powder on the tube wall is observed. The pyrolysis product is found to be in the form of porous lump. The colour of the lumps is black and most of the lumps are partially covered with fine white powder. The as synthesized product is found to be lumpy and fragile. The fragility increases with the NaCl addition. The powder is characterized by using X-ray diffractometer with Cu-Kα (λ=1.54 Å) radiation.

The amount of ZrO₂ is calculated from the XRD results and then the leached powder is mixed with calculated amount of Mg and H₃BO₃. Now this mixture is subjected to further synthesis in inert atmosphere and leaching is done as per first synthesis. Hereafter, we call the first and second synthesis as single SHS (SSHS) and double SHS (DSHS) respectively.

The phase analysis of DSHS powder is performed by XRD technique. The particle size distributions of different samples are determined by using particle size analyzer (Malvern Instruments Ltd., UK) with the help of laser scattering technique by dispersing the samples in alcohol. Morphology of the powders was characterized by scanning electron microscope (SEM)

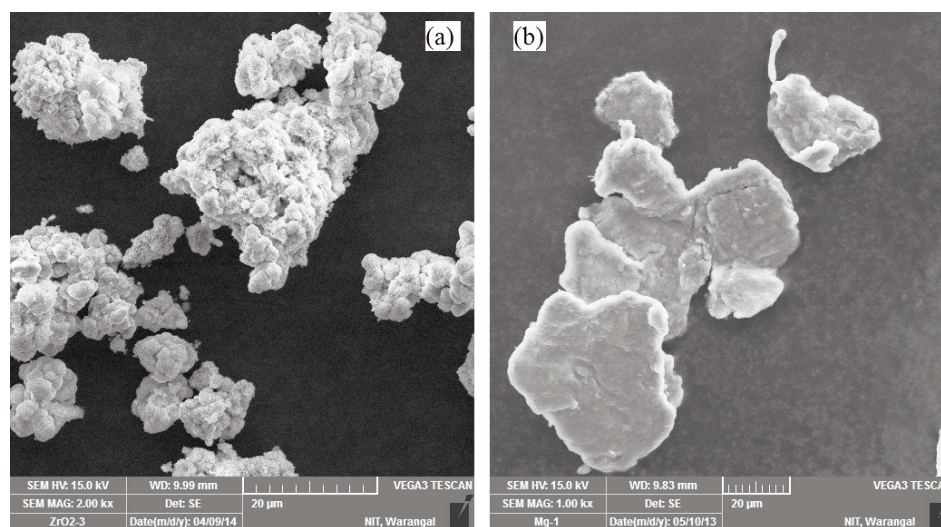


Figure 1. SEM micrographs of raw materials: (a) ZrO_2 and (b) Mg powder

(TESCAN, VEGA3 LMU VG9231273IN) equipped with EDS system. The resultant powders are analyzed further by using transmission electron microscope (TEM) (TECNAI G2) operated at 200kV and equipped with EDS system. The stoichiometric mixture of ZrO_2 -Mg and H_3BO_3 -Mg are heated upto 1000 °C in an inert atmosphere and the phase analysis of unleached and leached powder is carried out.

3. Results and discussion

The as-synthesis lumps were found in the tube and there was deposition of fine white powder on the tube wall. The colour of the lumps is black and most of the lumps are partially covered with fine white powder. The SEM image of fine white powder is shown in Fig. 2.

It shows presence of agglomeration of fine spherical particles. The EDS of powder shows presence of mainly magnesium and oxygen and other minor elements. The SEM/EDS has limitation to detect oxygen, boron and carbon etc. The Mg peak indicates that these powders are mainly of MgO phase.

The as synthesized product is found to be lumpy and fragile. The fragility increases with the NaCl addition. These lumps are ground and leached in dilute HCl for purification.

The XRD patterns of sample produced by SHS process using different amounts of NaCl is shown in Fig. 3. The XRD results show the presence of ZrB_2 as major phase with unreacted ZrO_2 as minor phase. By considering the highest intensity peaks of two phases, the amount of ZrB_2 and ZrO_2 is calculated as 87% and 13% respectively.

The XRD patterns indicate extensive line broadening for the NaCl added samples. The leached

and dried samples show ZrB_2 as the major phase with ZrO_2 as minor peak in all cases. The XRD patterns indicate extensive line broadening for the NaCl added samples. The broadening of (101) peaks (highest intensity at 42.2°) of ZrB_2 and the instrument line broadening of 0.2° is used for the calculation of average crystallite sizes, D, using the Scherrer formula, (ignoring the defect or strain contribution) [22].

$$D = \frac{0.9\lambda}{\beta_c(2\theta)\cos\theta} \quad (2)$$

Where, $\beta_c(2\theta)$ is the corrected broadening of the diffraction line measured at half the maximum intensity for the peak that appeared at the Bragg angle 2θ and λ is the corresponding wavelength of the X-ray radiation. The line broadening is corrected by using the following expression [22].

$$\beta_c^2(2\theta) = \beta_o^2(2\theta) - \beta_i^2(2\theta) \quad (3)$$

In the above equation, $\beta_o(2\theta)$ is the observed line broadening of the peak and $\beta_i(2\theta)$ is the measured value of the instrumental line broadening at the same angle 2θ . The crystallite sizes calculated for the powders are presented in Table 1. Addition of NaCl

Table 1. Effect of SHS diluent on the crystallite size of ZrB_2 powder

Sample No.	NaCl (wt%)	Angle (°2θ)	Broadening (°β)	Crystallite Size (nm)
A	0	42.2	0.212	41
B	10	42.2	0.231	30
C	20	42.2	0.254	25
D	DSHS	42.2	0.263	20

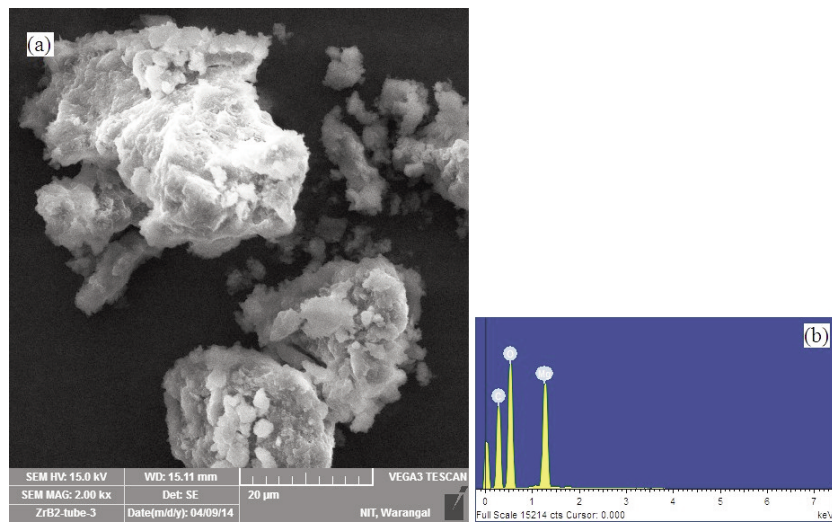


Figure 2. Morphology of white powder collected at the walls of the tube
(a) SEM image of powder and (b) EDS of the powder

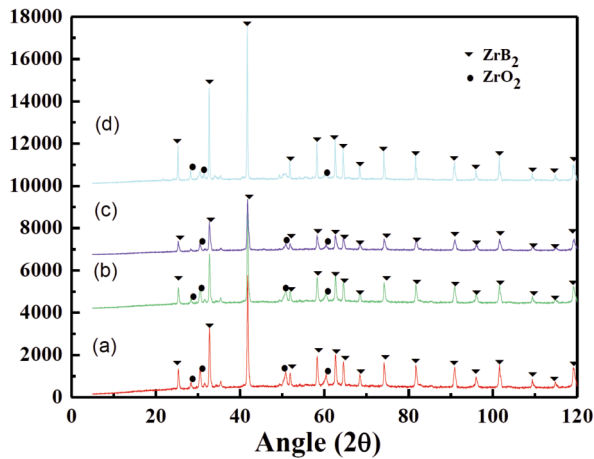


Figure 3. XRD patterns of different samples: (a) Sample A (0% NaCl), (b) Sample B (10% NaCl), (c) Sample C (20% NaCl) and (d) Sample D

seems to decrease the average crystallite size considerably.

The powder synthesized by using DSHS method contains lesser amount of ZrO_2 as compared to when it is synthesized initially. The amount of ZrB_2 and ZrO_2 is calculated as 94 % and 6 % respectively.

Determination of the particle size distributions of different samples reveal that the average particle size of sample A (0 wt% NaCl), B (10 wt% NaCl) and C (20 wt% NaCl) are 11.12, 8.21, and 7.42 μm respectively (Fig. 4a, b, and c). This indicates a decrease of particle size with the addition of NaCl. Although trends in the variation of sizes of the particles may be indicated with reasonable accuracy by this technique, but the accurate determination of the particle sizes is extremely difficult due to agglomeration of the particles [23].

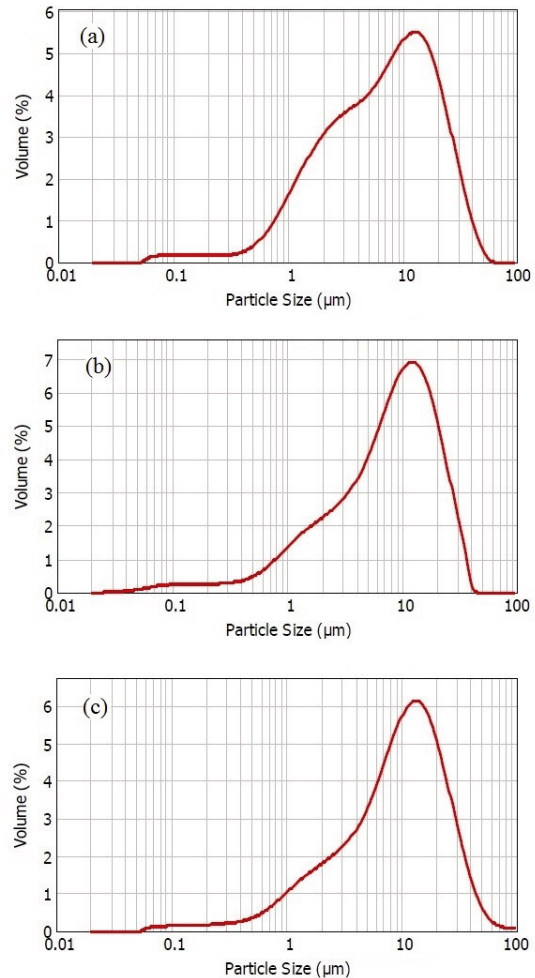


Figure 4. Particle size distribution of SHS synthesized (a) Sample A (0% NaCl), (b) Sample B (10% NaCl) and (c) Sample C (20% NaCl)

The SEM images of sample A are shown in Fig. 5. The unleached powder shows presence of agglomeration of spherical particles. Presence of agglomeration of particles is observed in the case of leached powder. The morphology of the synthesized powder for sample B and C (10% and 20% NaCl respectively) are shown in Figs 6 and 7. The unleached powder shows agglomeration of fine particles in both the cases, leached powder shows the presence of agglomeration of spherical particles. The morphology of the synthesized powder for sample D (DSHS) is shown in Fig.8, the unleached powder shows agglomeration of fine particles in both the cases.

The TEM images of ZrB_2 powder leached variously with NaCl are shown in Fig.9. Presence of ZrB_2 phase in nano crystalline form is confirmed by the presence of ring patterns in the selected area diffraction patterns (SAD) shown in the insets of Figs 9a, c and d. The TEM images of sample B (Fig. 9b) shows the formation of individual particles, which clearly defines the morphology and size of the particle. The morphology of the ZrB_2 in all the samples, as revealed by the TEM images, appears to be spherical and hexagonal. It may be noted that, after the SHS process, formation of crystalline structure, as revealed by the ring patterns in SADP's, is seen in the resultant powder. It is found that the particle size decreases with the NaCl addition.

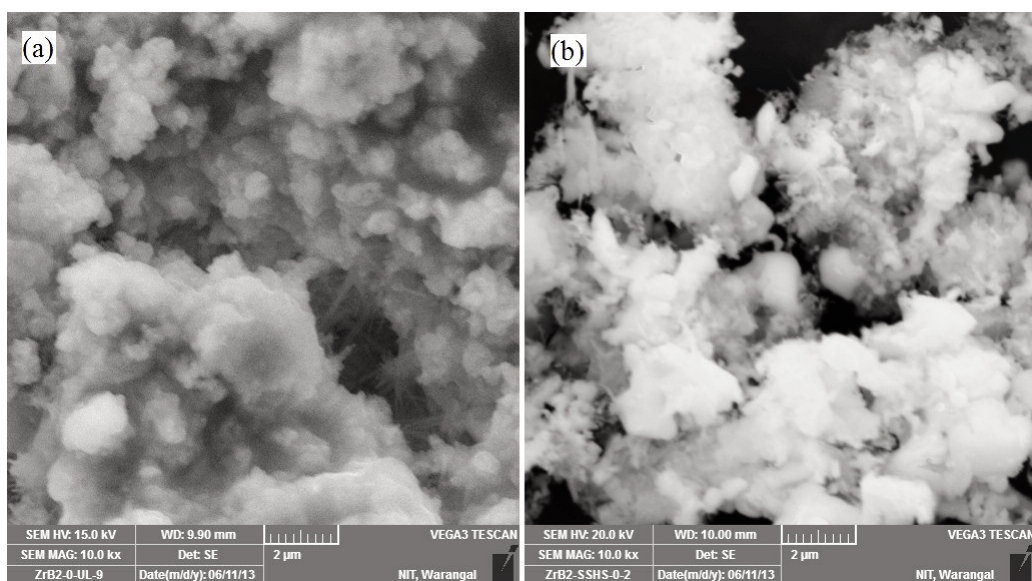


Figure 5. SEM images of sample A (0% NaCl): (a) - unleached powder and (b) - leached powder

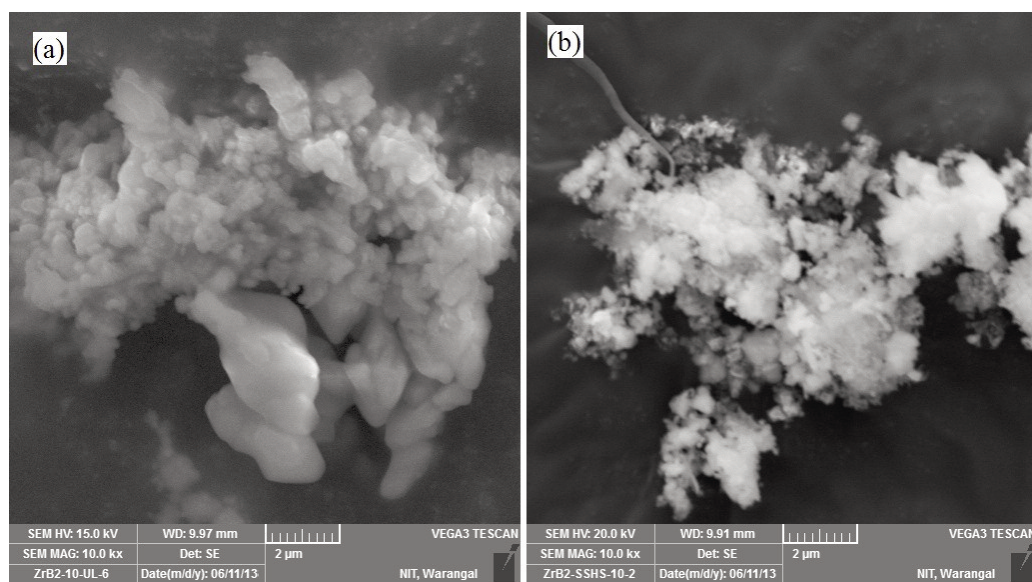


Figure 6. SEM images of sample B (10% NaCl): (a) - unleached powder and (b) - leached powder

The nature of explosion is much milder in case of NaCl addition and the intensity of explosion decreases with the increase of NaCl. The as synthesized product is found to be lumpy and fragile. The fragility increases with the NaCl addition. The melting and boiling point temperature of NaCl are 810°C and 1453°C respectively. The adiabatic temperature of the synthesis is around 2400°C, which indicates that some of the NaCl is vapourized during the synthesis and may result in the formation of a coating on the ZrB_2 particles. This coating may result in decreasing the growth rate of the particles. Presence of NaCl as a diluent may absorb heat which results in decreasing the adiabatic temperature. This phenomenon indicates

that the growth of ZrB_2 is occurred at lower temperature with respect to the synthesized powder when there is no addition of salt. A similar kind of phenomenon is noticed during the synthesis of TiB_2 powder [24].

The crystallite size of DSHS powder is found to be 20-60 nm. The TEM images of DSHS powder (Fig. 9d) reveal the formation of nanocrystalline powder (20-60 nm). This phenomenon indicates that there is decrease of particle size after DSHS. The presence of ZrB_2 in the reactant mixture acts as a diluent which could absorb heat during the synthesis (DSHS). As a result, the adiabatic temperature of the DSHS may decrease, which indicates that the synthesis

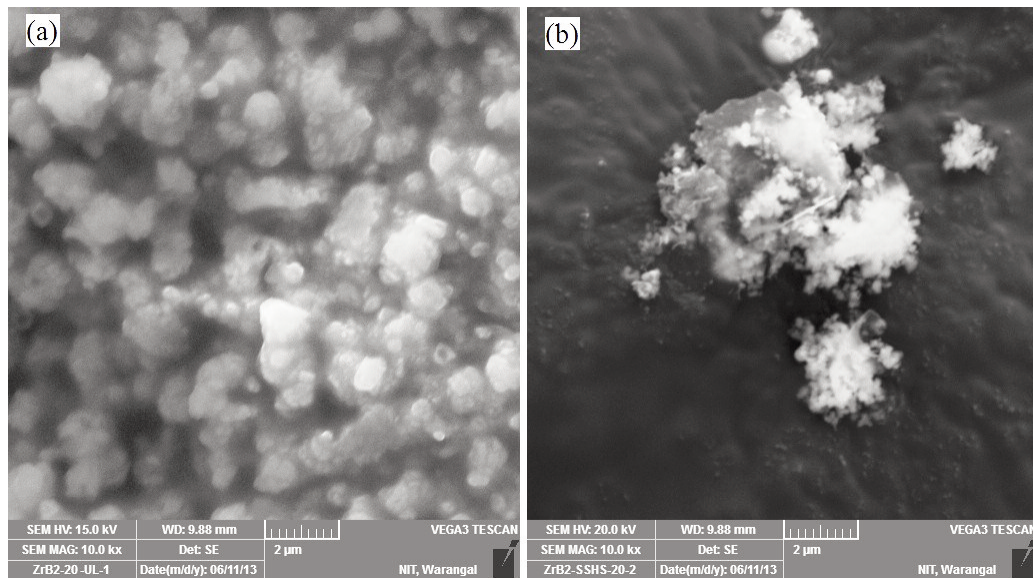


Figure 7. SEM images of sample C (20% NaCl): (a) - unleached powder and (b) - leached powder

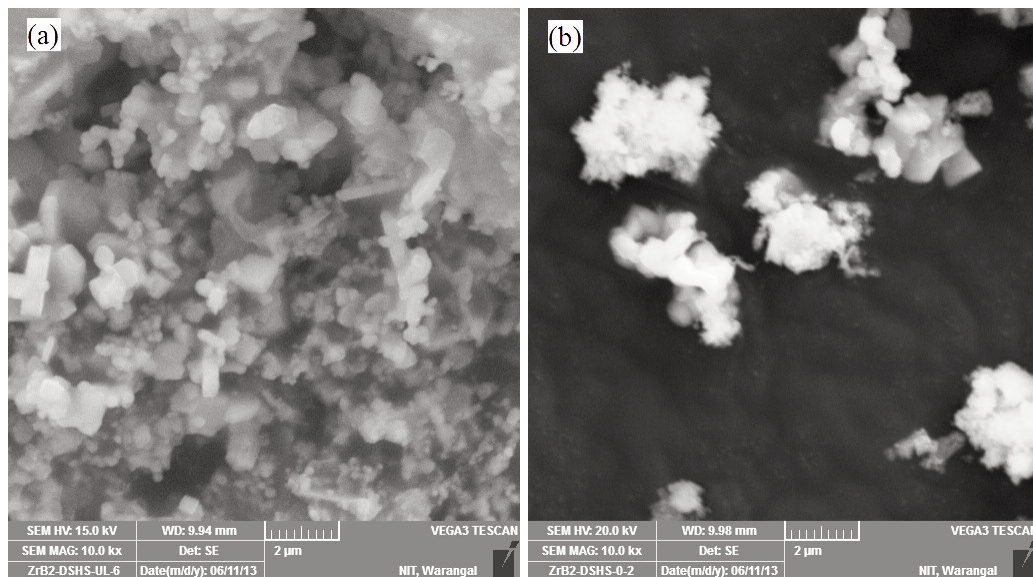


Figure 8. SEM images of sample D (DSHS): (a) - unleached powder and (b) - leached powder

may occurs at lower temperature. The decrease of unreacted ZrO_2 phase in the DSHS powder indicates the improvement in purity of powder after double synthesis. Attempt was there for further synthesis but there was no ignition. The details of DSHS mechanism is under investigation.

The XRD pattern of ZrO_2 -Mg system is shown in Fig.10. The unleached powder mainly contains MgO and Zr phase, whereas the leached powder shows elemental Zr and ZrO_2 phase. The XRD pattern of H_3BO_3 -Mg system (Fig. 11) shows presence of MgO as a major phase with Mg in the as synthesized powder. The XRD pattern of leached powder shows MgB_2 and MgB_4 as a minor phase respectively. The

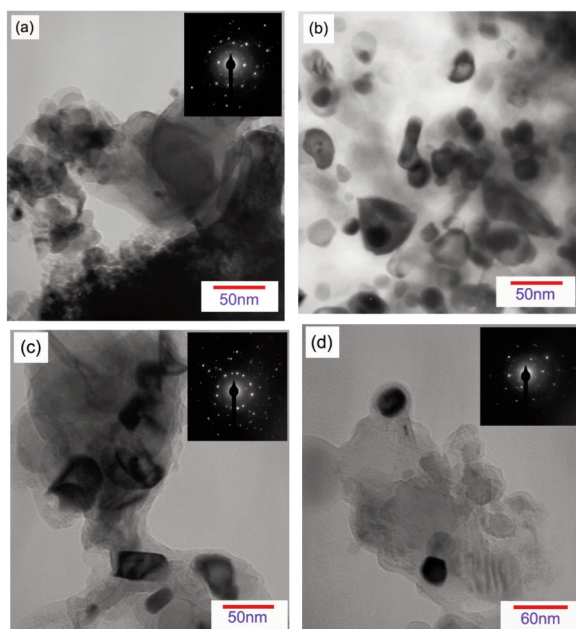


Figure 9. TEM images of leached sample: (a) Sample A (0% NaCl), (b) Sample B (10% NaCl), (c) Sample C (20% NaCl), and (d) Sample D

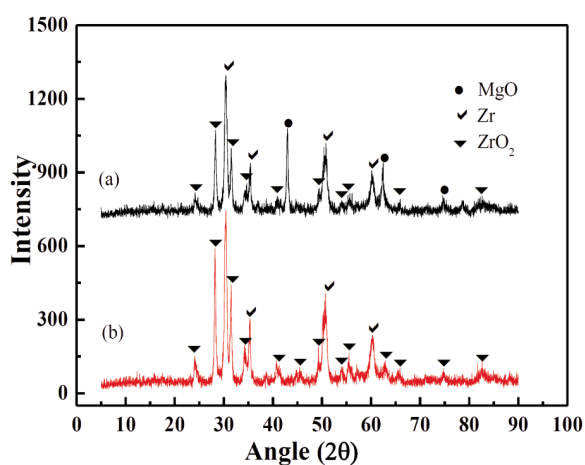


Figure 10. XRD patterns of ZrO_2 -Mg system: (a) and (b) are unleached and leached powder

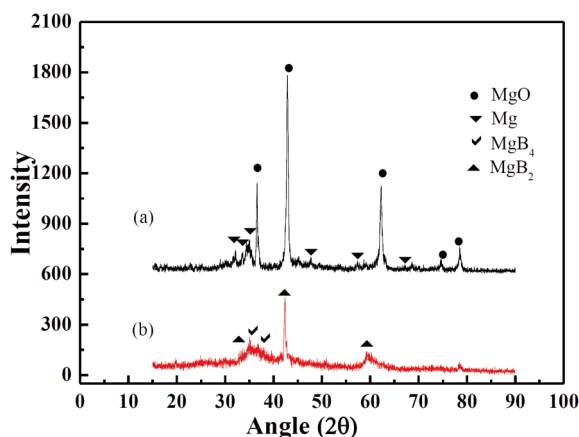


Figure 11. XRD patterns of H_3BO_3 -Mg system: (a) and (b) are unleached and leached powder

presence of boron is not detected, which could be due to lower amount of boron formation.

4. Conclusions

The nanocrystalline ZrB_2 powder can be produced through SHS process by using inexpensive raw materials. The XRD results of SSSH powder show the presence of ZrB_2 as major phase with ZrO_2 (unreacted) as minor phase. The particle size of ZrB_2 decreased with the addition of NaCl as SHS diluent. The SEM images show the presence of agglomeration of fine spherical particles. The TEM analysis of powder shows decrease of particle size after DSHS and particles are in nano metric scale. The particles are decreased with the addition of NaCl as diluent. The DSHS reaction has reduced the formation of unreacted oxide in the resultant powder.

Acknowledgements

Authors would like to thank Dr. Amol A. Gokhale, Director, DMRL and Dr. Ghoshal, Group Head, Electron Microscopy Group, DMRL, for providing permission to carry out TEM investigations.

References

- [1] H. E. Camurlu and F. Maglia, J. Eur. Ceram. Soc. 29 (8) (2009) 1501–1506.
- [2] E. Y. Jung, J. H. Kim, S. H. Jung, and S. C. Choi, J. Alloys Compd. 538 (2012) 164–168.
- [3] J. W. Zimmermann, G. E. Hilmas, and W. G. Fahrenholtz, Mater. Chem. Phys. 112 (2012) 140–145.
- [4] Y. Li, W. Han, H. Li, J. Zhao, and T. Zhao, Mater. Lett. 68 (2012) 101–103.
- [5] M. Patel, J. J. Reddy, V. V. Bhanu Prasad, J. Subrahmanyam, and V. Jayaram, Mater. Sci. Eng. A. 535 (2012) 189–196.
- [6] H. T. Liu, J. Zou, D. W. Ni, W. W. Wu, Y.M. Kan, and

- G. J. Zhang, *Scr. Mater.* 65 (2011) 37–40.
- [7] B. Li, J. Deng, and Y. Li, *Int. J. Refract. Met. Hard Mater.* 27 (4) (2009) 747–753.
- [8] S. Zhang, S. Wang, W. Li, Y. Zhu, and Z. Chen, *Mater. Lett.* 65 (19) (2011) 2910–2912.
- [9] N. Setoudeh and N. J. Welham, *J. Alloys Compd.* 420 (2006) 225–228.
- [10] Y. Zhang, R. Li, Y. Jiang, B. Zhao, H. Duan, J. Li, and Z. Feng, *J. Solid State Chem.* 184 (8) (2011) 2047–2052.
- [11] B. Akgün, H. E. Çamurlu, Y. Topkaya, and N. Sevinç, *Int. J. Refract. Met. Hard Mater.* 29 (5) (2011) 601–607.
- [12] D. W. Ni, G. J. Zhang, Y. M. Kan, and Y. Sakka, *Scr. Mater.* 60 (8) (2009) 615–618.
- [13] M. A. Karsh and R. A. Ayers, *Int. J. of Self-Propagating High Temp. Syn.* 20 (3) (2011) 143–149.
- [14] Y. H. Kang, L. Wang, L. C. Fu, J. Yang, Q. L. Bi, and W. M. Liu, *Int. J. of Self-Propagating High Temp. Syn.* 20 (2) (2011) 134–139.
- [15] I. P. Borovinskaya, V. N. Semenova, and I. D. Kovalev, *Int. J. of Self-Propagating High Temp. Syn.* 20 (2) (2011) 113–117.
- [16] W. W. Wu, G. J. Zhang, Y. M. Kan, and P. L. Wang, *Mater. Lett.* 63 (16) (2009) 1422–1424.
- [17] A. R. Kamali, M. R. Aboutalebi, and M. R. Farhang, *Int. J. of Self-Propagating High Temp. Syn.* 17 (4) (2008) 233–236.
- [18] U. Demircan, B. Derin, and O. Yucel, *Mater. Res. Bull.* 42 (2) (2007) 312–318.
- [19] P. Mossino, *Ceramics International.* 30 (3) (2004) 311–332.
- [20] G. H. Liu, J. T. Li, and K. X. Chen, *Advances in Applied Ceramics.* 112 (3) (2013) 109–124.
- [21] J. K. Sonber and A. K. Suri, *Advances in Applied Ceramics.* 110 (6) (2011) 321–334.
- [22] B. D. Culity, Addison-Wesley Publishing Company. (1997) 102-121.
- [23] P. Pourghahrsamani, E. Forssberg, *Mineral Processing and Extractive Metallurgy Review.* 26 (2005) 145-166.
- [24] Gadakary Saikumar, Asit K. Khanra, and R. Veerabau, *Advances in Applied Ceramics.* 113 (7) (2014) 419-426.